COMMUNICATION

Photoactive carbon monoxide-releasing coordination polymer particles

Received 00th January 20xx,
Accepted 00th January 20xx

DOI: 10.1039/x0xx00000x

Arnau Carné-Sánchez,*[,a,b] Shuya Ikemura,[a,d] Reiko Sakaguchi,[a] Gavin A. Craig,*[,a,c] Shuhei Furukawa*[,a,d]

We report the synthesis of photoactive carbon monoxide-releasing coordination polymer particles through the assembly of Mn(I) carbonyl complexes with bis(imidazole) ligands. The use of Mn(I) carbonyl complexes as metallic nodes in the coordination network avoids the potential for aggregation-induced self-quenching, favouring their use in solid-state.

The discovery of the biological role of carbon monoxide (CO) as a gasotransmitter and its beneficial physiological effects in multiple processes such as vasodilation, anti-inflammation, antiproliferation and anti-apoptosis have opened an era of research devoted to using CO as a therapeutic drug.[1,2] However, gaseous CO is also known for its lethal toxicity especially when it is accumulated in the lungs at a high concentration. Therefore, the feasibility of using CO as a therapeutic drug relies on the ability to control its release to targeted tissues, organs and blood vessels. In this context, materials that are able to store CO in the solid state and liberate it upon an external stimulus are highly pursued.[3] Light is a suitable trigger to release CO because it enables control of the location, dosage and rate of CO release. Accordingly, photoactive CO-releasing materials (photoCORMAs) have been extensively studied.[4] The two main current strategies to synthesise photoCORMAs are the surface functionalization of photoactive CO-donor molecules on inorganic[5–7] and organic nanoparticles[8–10] and the encapsulation of such photoactive CO-donor molecules within the cavities of porous materials.[11–14]

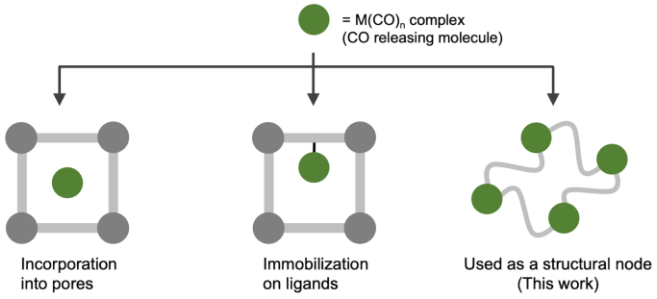

Figure 1. Illustration of the current strategies to immobilize photoactive CO-releasing complexes in coordination networks.

Herein, we report a novel strategy based on using a photoactive CO-releasing complex, in this case, a manganese(I) carbonyl complex, as a metallic node in the synthesis of amorphous coordination polymers. To this end, we polymerized Mn(I) carbonyl complexes through the coordination bond formation with bis(imidazole) ligands to yield amorphous coordination networks as CO-releasing coordination particles (CORPs). Spectroscopic characterization of the CORPs show that the integrity of the photoactive $Mn(CO)_3$ moiety is maintained upon polymerization. Furthermore, the photo-triggered CO releasing studies performed in the solid-state reveal that the $Mn(CO)_3$ centres remain active within the amorphous networks. Finally, we tune the CO-releasing performance of CORPs through meso- and molecular-scale modifications by downsizing the coordination particles and enhancing the inter-$Mn(CO)_3$ distance, respectively.

Our strategy to incorporate a photoactive CO-releasing moiety as a building block in the synthesis of coordination polymer particles entails the use of manganese carbonyl complexes as metallic nodes and bis(imidazole) molecules as linkers (Figure 1). This synthetic strategy benefits from the inherent photo-triggered CO releasing property of the manganese carbonyl complexes and the relatively strong N-Mn coordinate bond.[15–18] As a bridging ligand, we initially chose 1,4-bis(imidazol-1-ylmethyl)benzene (bix) because its flexibility

[a.] *Institute for Integrated Cell-Material Sciences (WPI-iCeMS), Kyoto University, Yoshida, Sakyo-ku, Kyoto 606-8501, Japan.*
[b.] *Catalan Institute of Nanoscience and Nanotechnology (ICN2) CSIC and The Barcelona Institute of Science and Technology Campus UAB, Bellaterra, 08193 Barcelona, Spain.*
[c.] *Department of Pure and Applied Chemistry, University of Strathclyde, G11XL Glasgow, Scotland.*
[d.] *Department of Synthetic Chemistry and Biological Chemistry, Graduate School of Engineering, Kyoto University, Katsura, Nishikyo-ku, Kyoto 615-8510, Japan*

Electronic Supplementary Information (ESI) available: Detailed synthesis and characterization methods. See DOI: 10.1039/x0xx00000x

This is a peer reviewed, accepted author manuscript of the following research article: Carné-Sánchez, A., Ikemura, S., Sakaguchi, R., Craig, G. A., & Furukawa, S. (2022). Photoactive carbon monoxide-releasing coordination polymer particles. Chemical Communications, 58(71), 9894-9897. https://doi.org/10.1039/D2CC03907A

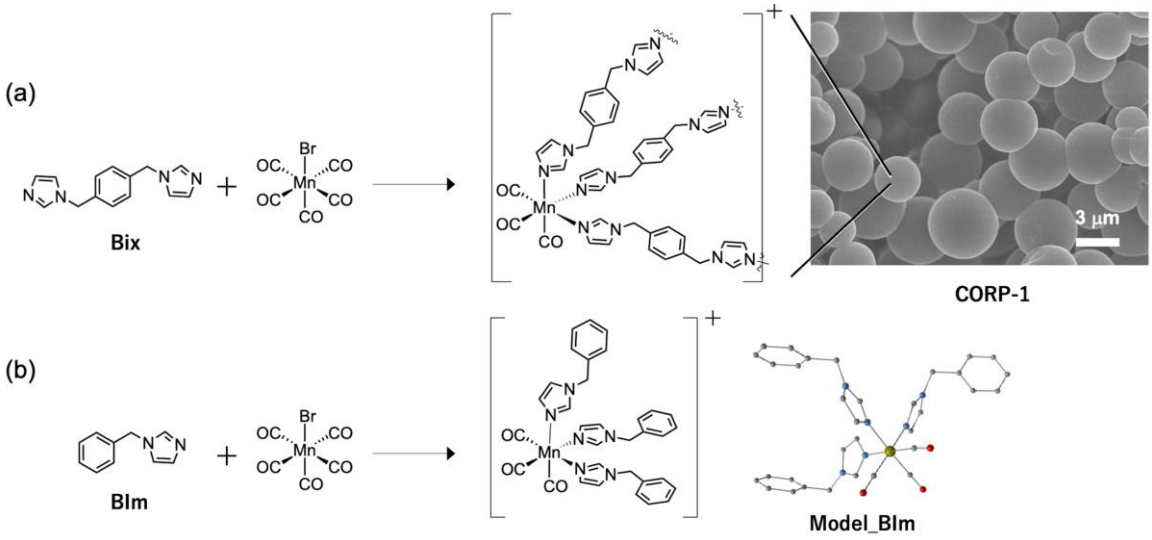

Figure 2. (a) Coordination polymerization reaction to yield CORP-1 in the form of micrometric spherical particles (right). (b) Coordination reaction to yield the model compound related to CORP-1 in the form of a crystalline molecular complex (right). The Br^- ion that balances the charge for the compounds is omitted from the schemes.

facilitates the formation of amorphous coordination particles.[19] Thus, $BrMn(CO)_5$ (36.5 mM) was reacted with 1.5 mol. eq. of bix (54.5 mM) in acetone at 65ºC for 12 hours to yield a colloidal suspension. The yellow solid was recovered by centrifugation and analysed by scanning electron microscopy (SEM): spherical particles with an average size of 3 μm (Figure 2a). This material is hereafter named as a CORP-1 (CORP = CO-releasing coordination particle).

The amorphous state of CORP-1 hinders the elucidation of its structural features at atomic level by conventional X-ray diffraction techniques. To overcome such limitations, one can employ X-ray absorption and pair distribution function (PDF) analysis to infer the electronic state and the local structure of the metal ions involved in the coordination network, respectively. Such techniques become even more powerful when the acquired spectra of the amorphous networks can be compared to a related crystalline compound used as a reference. Therefore, we synthesised a crystalline model compound related to CORP-1 by replacing the bidentate bix linker by the monodentate 1-benzylimidazole (BIm) ligand in the reaction with $BrMn(CO)_5$ (Figure 2b). This reaction yielded a discrete molecular complex with formula $[(BIm)_3Mn(CO)_3]Br$ (**Model_BIm**) as determined by single-crystal X-ray diffraction (Figure 2b). Thus, the reaction between $BrMn(CO)_5$ and BIm proceeds through the expected ligand exchange reaction, in which one Br- and two CO are replaced by three BIm molecules. The imidazole ligands coordinate to Mn(I) in a facial configuration and the released Br anion acts as a counter-ion to balance the positive charge of the Mn(I) complex.

Next, we employed the spectroscopic characterization of **Model_BIm** as a reference to elucidate the local structure of CORP-1. FT-IR analysis of **Model_BIm** and CORP-1 show similar CO stretching vibrations at 2030 and 1907 cm^{-1}, which confirms the presence of Mn(I) coordinated by CO ligands in CORP-1 (Figure S1). Solid-state UV-Vis diffuse reflectance spectroscopy revealed that the crystalline model compound and CORP-1 have a broad MLCT band in the 350 – 500 nm region, ascribed to a metal-to-ligand charge transfer (MLCT) transition band, from the manganese centres to the imidazole ligands (Figure S2).

To further establish the coordination environment of the Mn(I) ions in CORP-1, we measured X-ray absorption spectroscopy and compared the spectrum with that of **Model_BIm**. As observed in Figure 3a, the spectrum of CORP-1 is fully coincident with the one obtained for **Model_BIm**, which indicates the similarity of both compounds in their oxidation state and the coordination environment of the Mn(I) ions. PDF measurements performed on CORP-1 further supported the presence of Mn(I)-imidazole coordination bonds, as a peak at the distance corresponding to the Mn(I)-N bond is observed at 2.07 Å. The peak at 1.8 Å also suggests the presence of Mn(I)-CO coordination in the CORP-1 network (Figure S4). Taken together, the spectroscopic data for CORP-1 and **Model_BIm** indicate that the manganese-carbonyl complex in both compounds share the same coordination environment, local structure and oxidation state. Therefore, the coordination network of CORP-1 can be described as a 3-connected $Mn(CO)_3$ node bridged by bix linkers to give rise to a compound with the following formula $[Mn(bix)_{1.5}(CO)_3]_nBr_n$.

Once the structure of CORP-1 was elucidated, its CO-releasing capabilities were studied. First, we confirmed that CORP-1 does not release CO in the absence of light even when it is incubated in PBS buffered aqueous media for one day (Figure S5). Next, the photo-triggered CO release from CORP-1 in the solid-state was studied by infrared and UV-Vis spectroscopies. The IR spectrum of the sample subsequent to irradiation (UV light, 370 nm, 3.7 mW cm^{-1}) showed a significant decrease of the CO stretching vibration bands (Figure S6). Similarly, the MLCT absorption band at 350 – 500 nm progressively vanished under the same light exposure (Figure S7). On the other hand, **Model_BIm** did not display any spectroscopic changes upon light irradiation in the solid-state and only showed photo-triggered CO release in solution (Figure

S8). The amount of CO released as a function of the irradiation time was quantified by a customized in-line CO detector (Figure S9). Immediately after irradiating CORP-1 in the solid-state with UV light, it started releasing CO with a steady increase, reaching a saturation limit at *ca.* 1 mol CO per manganese ion (1.66 mmol CO/g of CORP-1), which translates into an average photo-release efficiency of 32 % (Figure 3b). In contrast, the molecular complex **Model_BIm** only released 0.23 mmol of CO per manganese ion after irradiation of a sample in the solid-state, which indicates that the photo-release efficiency of this compound in the solid-state is only 8% (Figure 3b).

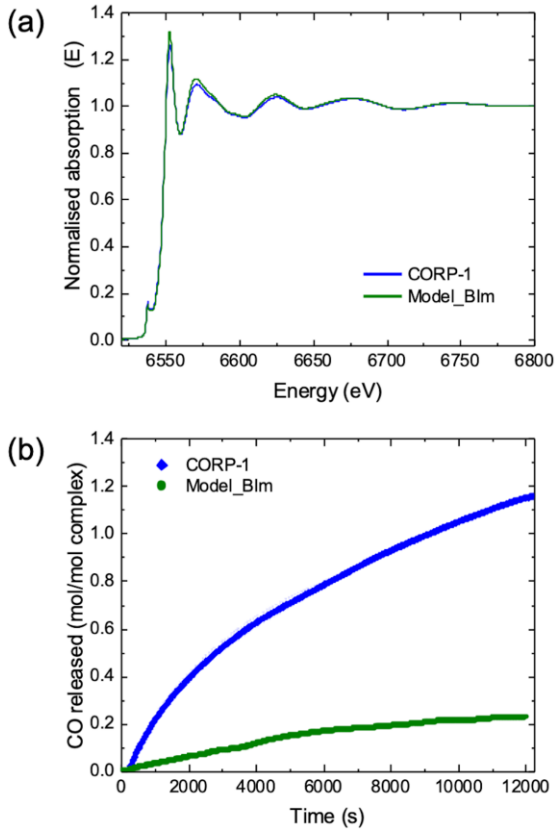

Figure 3. (a) EXAFS spectroscopic data of CPRP-1 and its related model compound, **Model_BIm**. (b) Time-dependent CO-release profile for CORP-1 and **Model_BIm** in the solid-state.

The improved photo-triggered CO-release properties of CORP-1 with respect to **Model_BIm** must be attributed to the network structure of the former because the local structure of the photoactive Mn(I) complex is the same in both compounds. Specifically, we propose that the spatial segregation of the photoactive $Mn(CO)_3$ centres within the coordination network inhibits aggregation-induced quenching and enables them to release CO upon irradiation.[13] However, for the photo-triggered CO release process to be efficient, light irradiation must be able to reach the photoactive centres located within the network and the released CO must be able to exit the network to the environment. Considering these two aspects, we reasoned that the performance of CORP-1 could be improved by elongating the inter-$Mn(CO)_3$ distance and by reducing the size of the colloidal particles. Increasing the inter-$Mn(CO)_3$ distance would lead to the formation of less dense networks with minimized self-aggregation induced quenching, while downsizing the particles would enable greater light penetration of the particles. The combination of these effects should increase the photo-efficiency of the reaction and facilitate the diffusion of CO through the network.

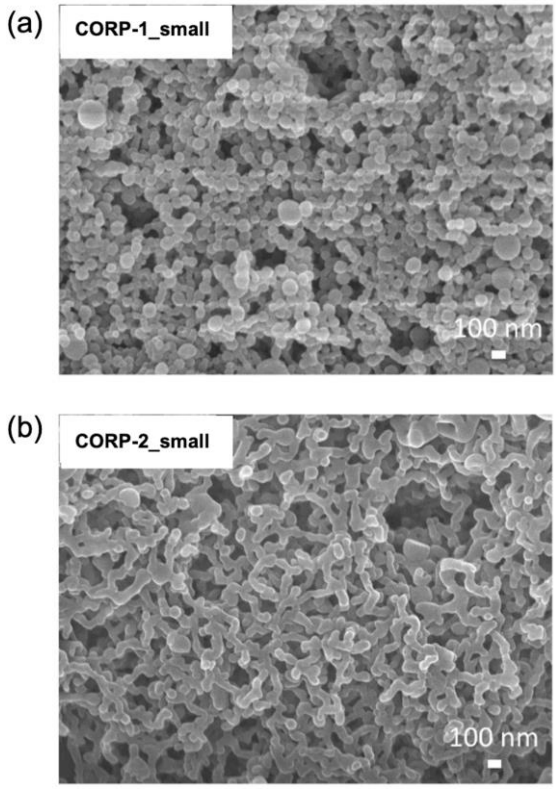

Figure 4. FESEM images of (a) CORP-1_small and (b) CORP-2_small.

Reducing the particle size of CORP-1 was approached by studying the effect of reactant concentration on the final size of CORP-1. These screening experiments revealed that the size of the CORP-1 particles decreased with the initial concertation of $BrMn(CO)_5$ and bix. Thus, when $BrMn(CO)_5$ and bix were reacted at a concentration of 9 mM and 13.8 mM, respectively, in acetone at 65ºC, colloidal particles of an average size of 200 nm were obtained (Figure 4a). These particles are hereafter named as CORP-1_small. The spectroscopic characterization performed on CORP-1_small, which includes FT-IR spectroscopy, X-ray adsorption and PDF analysis, confirmed that the structure of CORP-1_small is the same as CORP-1 (Figure S10 – S12). This characterization confirms that the miniaturization of the CORP-1 particles does not affect the local structure and electronic configuration of its constituents.

Next, we tuned the molecular scale structure of CORP-1 through ligand design. We used an extended version of the bix ligand, namely 4,4'-bis(imidazol-1-ylmethyl)biphenyl (hereafter named bpBix) as a bridging ligand between the $Mn(CO)_3$ nodes with the aim of increasing their spatial segregation. The reaction of bpBix (13.8 mM) and $BrMn(CO)_5$ (9 mM) in acetone at 65ºC yielded a colloidal suspension composed of spherical particles of ca. 200 nm, hereafter named as CORP-2_small (Figure 4b).

The spectroscopic characterization of CORP-2_small confirmed that the structure of the $Mn(CO)_3$ nodes is equivalent to the one

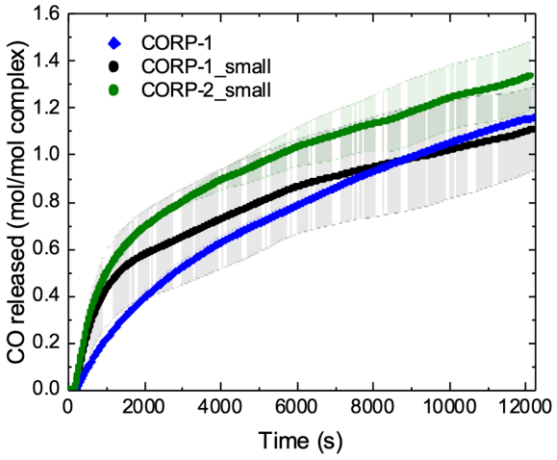

Figure 5. Time-dependent CO-release profile for CORP-1_small (black), CORP-1_large (blue) and CORP-2_small (green)

observed for CORP-1 and CORP-1_small (Figure S13 – S16).

The solid-state photo-triggered CO-releasing properties of CORP-1, CORP-1_small and CORP-2_small are presented in Figure 5. The CO releasing profile of the three samples highlights the impact of miniaturization on the kinetics of the solid-state CO release from the CORP-1 network as evidenced from the comparison of CORP-1 and CORP-1_small. Whereas CORP-1 releases half of the total CO released after 58 min of irradiation time, CORP-1_small releases the same percentage of CO after only 16 min of irradiation time. These results can be ascribed to the higher proportion of $Mn(CO)_3$ moieties on the surface of CORP-1_small when compared to CORP-1. However, the higher percentage of surface exposed photoactive centres does not translate into a significant increase of the total amount of CO released after the full irradiation time. This result can be ascribed to the fact that that the light penetration in CORP-1 and CORP-1 is similar and therefore the same number of photoactive centres are excited making the overall photo efficiency for both types of samples very similar. The comparison of CORP-1_small and CORP-2_small shed light on the impact of the molecular scale structural features of the coordination network. Both structures share a very similar CO-releasing curve at the early stages of the CO-releasing experiment. However, while the CO-release kinetics from CORP-1_small decelerates after exposing it to light for approximately 1 hour, CORP-2_small shows a steady linear increase of released CO after 1 hour of irradiation time. While the burst initial release of CO from CORP-1_small and CORP-2_small can be attributed to the activity of the surface $Mn(CO)_3$ centres, the linearly sustained CO release at long irradiation times observed in the case of CORP-2_small might be ascribed to the performance of the inner $Mn(CO)_3$ moieties. This phenomenon translates into a higher photo efficiency of CORP-2_small (44%) over CORP-1_small (38%). Therefore, we postulate that increasing the segregation between the metallic centres in the coordination network does not only limit the extent of aggregation-induced quenching but also makes the network less dense, which facilitates CO release from the inner core of the particle.

In conclusion, we have shown that the photoactive complex $Mn(CO)_3$ can be employed as a metallic node in coordination networks and that through this approach they become responsive upon light irradiation in solid-state. Therefore, the results presented here open the way to the design of new amorphous CORMAs with high payloads of CO and increased processability.

Conflicts of interest

The authors declare that there are no conflicts of interest in this publication

Acknowledgements

The synchrotron X-ray experiments were performed at the BL02B2 of SPring-8 with the approval of the JASRI (Proposal No. 2016B1126 and 2017A1180). The authors thank the iCeMS Analysis Center for access to analytical instruments.

References

1 L. Wu and R. Wang, *Pharmacol. Rev.*, 2005, **57**, 585.
2 R. Motterlini and L. E. Otterbein, *Nat. Rev. Drug Discov.*, 2010, **9**, 728–743.
3 D. Nguyen and C. Boyer, *ACS Biomater. Sci. Eng.*, 2015, **1**, 895–913.
4 A. C. Kautz, P. C. Kunz and C. Janiak, *Dalton Trans.*, 2016, **45**, 18045–18063.
5 G. Dördelmann, H. Pfeiffer, A. Birkner and U. Schatzschneider, *Inorg. Chem.*, 2011, **50**, 4362–4367.
6 Q. He, D. O. Kiesewetter, Y. Qu, X. Fu, J. Fan, P. Huang, Y. Liu, G. Zhu, Y. Liu, Z. Qian and X. Chen, *Adv. Mat.*, 2015, **27**, 6741–6746.
7 W.-P. Li, C.-H. Su, L.-C. Tsao, C.-T. Chang, Y.-P. Hsu and C.-S. Yeh, *ACS Nano*, 2016, **10**, 11027–11036.
8 P. Govender, S. Pai, U. Schatzschneider and G. S. Smith, *Inorg. Chem.*, 2013, **52**, 5470–5478.
9 D. Nguyen, N. N. M. Adnan, S. Oliver and C. Boyer, *Macromol. Rapid Commun.*, 2016, **37**, 739–744.
10 R. Sakla and D. A. Jose, *ACS Appl. Mater. Interfaces*, 2018, **10**, 14214–14220.
11 F. J. Carmona, C. R. Maldonado, S. Ikemura, C. C. Romão, Z. Huang, H. Xu, X. Zou, S. Kitagawa, S. Furukawa and E. Barea, *ACS Appl. Mater. Interfaces*, 2018, **10**, 31158–31167.
12 F. J. Carmona, I. Jiménez-Amezcua, S. Rojas, C. C. Romão, J. A. R. Navarro, C. R. Maldonado and E. Barea, *Inorg. Chem.*, 2017, **56**, 10474–10480.
13 S. Diring, A. Carné-Sánchez, J. Zhang, S. Ikemura, C. Kim, H. Inaba, S. Kitagawa and S. Furukawa, *Chem. Sci.*, 2017, **8**, 2381–2386.
14 A. Carné-Sánchez, F. J. Carmona, C. Kim and S. Furukawa, *Chem. Commun.*, 2020, **56**, 9750–9766.
15 M. A. Wright and J. A. Wright, *Dalton Trans.*, 2016, **45**, 6801–6811.
16 M. A. Gonzalez, S. J. Carrington, N. L. Fry, J. L. Martinez and P. K. Mascharak, *Inorg. Chem.*, 2012, **51**, 11930–11940.

17 I. Chakraborty, S. J. Carrington and P. K. Mascharak, *Acc. Chem. Res.*, 2014, **47**, 2603–2611.
18 J. Niesel, A. Pinto, H. W. P. N'Dongo, K. Merz, I. Ott, R. Gust and U. Schatzschneider, *Chem. Commun.*, 2008, 1798–1800.
19 I. Imaz, J. Hernando, D. Ruiz-Molina and D. Maspoch, *Angew. Chem. Int. Ed.*, 2009, **48**, 2325–2329.

…